

Sinus Elevation with a Cortical Bone Graft Block: A Patient-Specific Three-Dimensional Finite Element Study

Peter Schuller-Götzburg, MD, DDS¹/Karl Entacher, PhD, Univ-Doz²/Alexander Petutschnigg, PhD³/
Werner Pomwenger, DI (FH), MSc⁴/Franz Watzinger, MD, DDS, Univ-Doz⁵

Purpose: The aim of the present study was to perform a finite element (FE) analysis of a modified sinus elevation procedure involving additional implantation of a cortical bone graft block for stabilization of an implant. A secondary aim was to compare the modified sinus augmentation with the standard technique and to determine whether the FE model to replace a dental implant can be simplified into a cylinder without compromising the accuracy of the outcome. **Materials and Methods:** Based on computed tomography data, three-dimensional FE models of half of a maxilla were created. A basic model was generated to analyze a conventional sinus elevation procedure and another was created for the modified version, which involved insertion of a cortical bone graft block. Two implant models were used in the premolar region: a typical threaded endosseous dental implant and a simplified 4 × 10-mm cylinder. Occlusal loads were applied in axial, mediotrusive, and laterotrusive directions, and perfect bonding was assumed to be present at all interfaces. **Results:** The maximum von Mises stresses were significantly lower for the sinus graft models with added cortical bone than for the conventional sinus elevation under all types of loads. No significant difference was observed between the use of threaded implants and the simplified implant cylinders. **Conclusion:** The addition of a cortical bone graft may be a useful approach to decrease stresses around implants placed into the grafted sinus. INT J ORAL MAXILLOFAC IMPLANTS 2012;27:359–368

Key words: dental implant loading, finite element analysis, maxillary atrophy, sinus elevation, three-dimensional modeling

Implant rehabilitation of the partly edentulous or edentulous maxilla is limited by the quantity and quality of available bone. Conventional implant insertion is not feasible in many patients who may require augmentation procedures. In cases of atrophic alveolar bone in a posterior maxilla with pronounced sinus pneumatization, such as class V and VI,¹ elevation of the sinus membrane with subsequent augmentation of the subantral space (sinus bone graft) is a clinically proven and safe technique.² Various types of graft

materials, implants, and modified surgical methods have been proposed to improve the efficacy of the treatment.^{3–9} In addition, some clinical studies have examined the use of allogeneic¹⁰ or autogenous^{11–13} bone graft blocks for sinus augmentation.

Dual anchorage of implants in crestal bone and cortical bone provides ideal stabilization and fixation of the implants, minimizes losses during healing after the surgical procedure, and leads to better osseointegration of implants. Therefore, the aim of the present finite element (FE) study was to analyze and compare the stress around implants inserted following a standard sinus bone graft and following a modified procedure that employs a cortical bone graft block. Loading of dental implants in a highly atrophic posterior maxilla was simulated and assessed under various loading conditions. In addition, dental implants with two different geometries were designed to assess the value of complex FE models. The complex geometry of a commercially available dental implant (Sky Implant System, Bredent-Medical) was modeled, and the implants were then redesigned as pure cylinders (4 × 10 mm) without threads for the purpose of comparison. Three-dimensional (3D) FE analyses were carried out with and without placement of a cortical bone graft block for each of these two settings.

¹Head of Prosthetics, Biomechanics, and Biomaterial Research, Paracelsus Medical University, Salzburg, Austria.

²Associate Professor, Department of Information Technologies and Systems Management, Salzburg University of Applied Sciences, Austria.

³Head, Department of Forest Products Technology and Wood Construction, Salzburg University of Applied Sciences, Austria.

⁴Assistant Professor, Department of Information Technologies and Systems Management, Salzburg University of Applied Sciences, Austria.

⁵Head, Department of Maxillofacial Surgery, Landesklinikum St. Pölten–Lilienfeld, Austria.

Correspondence to: DDr Peter Schuller-Götzburg, Paracelsus Medical University, Prosthetics, Biomechanics, and Biomaterial Research, Strubergasse 21, A-5020 Salzburg, Austria. Fax: +43-662-880769. Email: peter.schuller-goetzburg@pmu.ac.at



Fig 1 CT image of a section of the maxilla shows the left sinus, augmented with particulated bone and the cortical bone graft block, which is held in place with two fixation screws.



Fig 2 3D model after automatic segmentation and manual refinement.

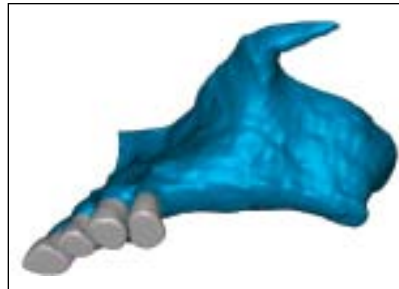


Fig 3 Final 3D surface model of the maxilla after the "wrapping" procedure.

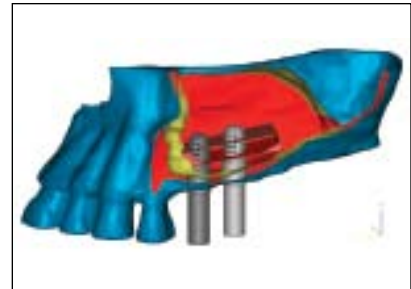


Fig 4 Complete surface model consisting of the maxilla, the augmented area, the bone graft, and the positioned implants.

MATERIALS AND METHODS

FE Model Design

A patient-specific 3D model of the left half of the maxilla with augmentation and a cortical bone graft block was generated based on actual computed tomography (CT) data from a patient. These patient-specific 3D FE models are more extensive versions of the models used in recent FE studies.^{14–18} A block from the retromolar region of the mandible was inserted in the sinus during augmentation of the maxillary sinus. In a first step, the sinus elevation was carried out using a cortical bone graft. The position of the bone graft block is in the upper third of the implant in the sinus. The graft was anchored on the crestal aspect with two fixation screws. The space between the bone block and the sinus floor was filled as usual with particulated autogenous/allogeneous bone material. Implants were placed 4 months later. The fixation screws were removed and the implants inserted. Thus, the fixation screws were used to position the implants and measure their length.

Figure 1 shows a patient after the modified sinus augmentation. The left part of the maxilla, bone graft, and bone augmentation material were segmented using Mimics software (Materialise). The images were preprocessed using a combination of automatic and manual segmentation methods, as automatic seg-

mentation alone does not yield adequate solutions for computation of a 3D model.¹⁵ The resulting 3D model was rather coarse and had several holes and defects because of the 1.25-mm slice thickness of the CT images (Fig 2). Owing to insufficient CT resolution, the bone graft was segmented loosely and remodeled later.

The aforementioned geometric inhomogeneities had to be resolved to achieve a suitable 3D model. A function provided by 3-matic software (Materialise) permits the investigator to wrap the entire geometry of an object in a simulated "cellophane" layer. All holes and defects were corrected by this procedure. The result was a smooth and homogenous surface that covered all anatomical elements (Fig 3). The thickness of the cortical sinus floor varied between 1 and 3 mm. The cortical bone graft block was remodeled to its known size of $17 \times 8 \times 2.5$ mm (as measured on the CT). Then, based on the CT images, the anterior portion of the remodeled cortical bone graft block was trimmed to fit into the sinus. The geometry of the 10-mm BlueSky4010 implant (Bredent Medical) was used for the dental implants. The implants were inserted in their correct anatomical and prosthetic positions and oriented to replace the second premolar and first molar in the left maxilla (Fig 4). The implants had a maximum diameter of 4 mm and a total length of 10 mm. Prosthetic abutments were then modeled as cylinders

Table 1 Model Specifications

Model	No. of elements	No. of nodes
With cortical bone graft block + threaded implant	584,155	107,552
Without cortical bone graft block + threaded implant	447,523	82,598
With cortical bone graft block + cylindric implant	583,692	107,617
Without cortical bone graft block + cylindric implant	409,397	76,230

measuring 3.6 mm in diameter and 9 mm in height over the implant shoulder, aligned to the axis, and fixed without any loosening.

A 3D model of volume elements is required for FE analysis. This was generated using the ICEM CDF software (Ansys), which consists of SOLID185 volume elements that are widely used to obtain a model of solid structures. Several parameters of the 3D model, such as maximum element size and element deviation, permit the investigator to regulate the meshing procedure of each 3D component. Boolean operations among the components were carried out using ICEM by means of permeation. This provided a mesh for the threaded and cylindric implants and the cortical bone graft block.

The networking procedure is rendered difficult by the complex geometry of the implants, and FE models are restricted by the number of elements and nodes. For the purpose of simplification, therefore, the threaded dental implant was replaced by a simple cylinder. Thus, four different models were used for simulation with different meshes (Table 1).

Material Properties

Various material parameters were used for the 3D FE models.¹⁵ The maxilla and the bone graft consisted of compact bone and were therefore categorized as cortical bone. The particulated bone augmentation material was defined as cancellous bone and the implants as titanium (Table 2). All of the materials were presumed to be homogenous, isotropic, and linearly elastic.

Interface Conditions

The model was presumed to represent ideal osseointegration, with 100% union between the augmented bone, implants, bone graft, and maxilla. The connections between implants and abutments were assumed to be completely bonded with no loosening.

Loading and Boundary Conditions

Ansys FE software (Ansys) was used for FE analysis. In keeping with the anatomy of the maxilla, it features a fixed bearing at the anterior and superior transverse cutting planes, allowing for no translational or rotational movement.

Table 2 Material Properties

Material	Young's modulus (MPa)	Poisson ratio
Cancellous bone	1,400	0.3
Cortical bone	14,000	0.3
Titanium	103,400	0.35

Masticatory forces in the *x*-, *y*- and *z*-axes formed the basis for the simulation of loads.¹⁹ In the *x*-axis, laterotrusion was presumed at 13 N, and in the *y*-axis, protrusion was assumed to be 36 N. For loading in the *z*-axis, 96 N was used as the axial masticatory force.

Von Mises stresses were calculated using the FE models. Because bone is an inhomogenous material, different stresses were used to assess the compact alveolar bone, the augmented material, and the bone block surrounding the implants. In addition, the distribution of stresses around and within the threaded dental implant and the simplified cylinder was compared.

RESULTS

FE simulations of von Mises stresses in all axes revealed maximum stresses near the cortical alveolar bone in the maxilla. Stresses in the cortical bone block graft were higher than those in the surrounding particulated bone, but they were significantly lower than those in the alveolar cortical bone area. This behavior was shown for all simulations.

Von Mises stresses in the *z*-axis, to simulate masticatory strength (Figs 5 to 9), showed that, independent of the implant type, models without a cortical bone block were marked by areas of significantly higher stresses around the implant neck in the cortical alveolar bone. Maximal stresses were higher in models with threaded implants (Figs 5 and 6) than in models with simplified cylindric implants (Figs 7 and 8), but the overall stress distributions were similar for both implant types.

Absolute maximum stresses were registered within the implants. Considering the maxilla alone, which absorbs maximum stress, the maximum von Mises

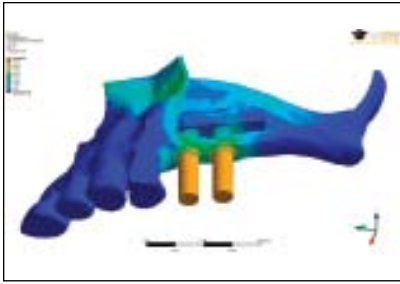


Fig 5 Distribution of von Mises stresses from z-load (masticatory strength) in the simulation with threaded implants and a cortical bone graft block. The maximum von Mises stress was 26.9 MPa.

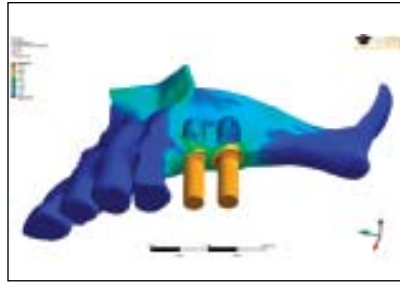


Fig 6 Distribution of von Mises stresses from z-load (masticatory strength) without a cortical bone graft block. Note the expanded area of stress in alveolar bone at the implant neck. The maximum von Mises stress is 20.7 MPa.

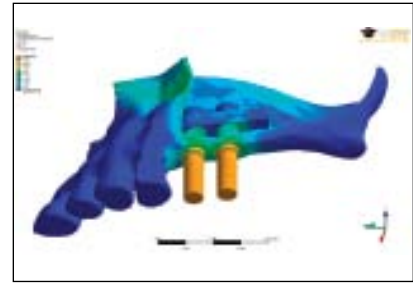


Fig 7 Distribution of von Mises stresses from z-load (masticatory strength) with cylindrical implants and an inserted cortical bone graft block. The maximum von Mises stress is 13.86 MPa.

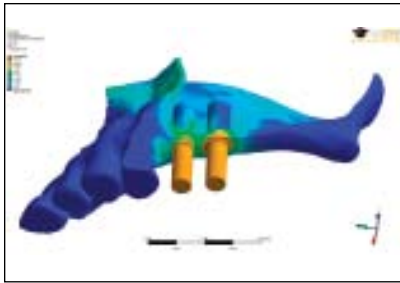


Fig 8 (Left) Distribution of von Mises stresses from z-load (masticatory strength) with cylindrical implants without insertion of a cortical bone graft block. The maximum von Mises stress is 19.76 MPa.

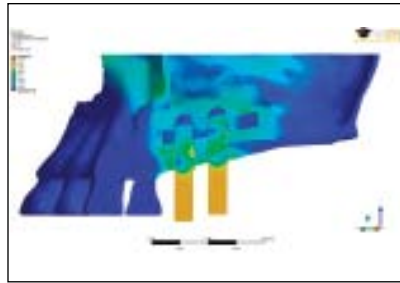


Fig 9 (Right) Sectional view of the distribution of von Mises stresses from z-load (masticatory strength) within threaded implants, the maxilla, and the cortical bone graft.

stresses were 8.3 MPa (Fig 5) with a cortical bone graft block and 20.2 MPa (Fig 6) without a cortical bone graft block for models with threaded implants. For models with simplified cylindrical implants, the maximum von Mises stresses were 11.78 MPa (Fig 7) with a cortical bone graft block and 17.55 MPa (Fig 8) without a cortical bone graft block (Table 3).

Without a cortical bone graft block, the stress distribution within the implant in the first molar area was roughly circular in all directions (Figs 6 and 8) at the implant neck, whereas high stresses were usually registered in the mesial and distal directions in models with a cortical block (Figs 5 and 7).

In a cross-sectional view of stresses within implants (Fig 9), the maxilla and the cortical bone graft block were seen to demonstrate certain singularities of the complex geometry of threaded implants. Models with cylindrical implant approximations were almost free of singularities and showed the same stress behavior as the models with threaded implants.

Analogous to masticatory strength, the distribution of von Mises stresses for the y-load condition (protrusion) was similar for the different implant models. Maximal stresses were 78.8 MPa for the cylinder (Fig 10) and 83.1 MPa for the threaded implant (Fig 11) without a cortical bone graft block. Maximal stress values in the surrounding alveolar bone were seen mesial to the first molar and were 31.55 MPa for the cylindrical implant (Fig 10) and 38.17 MPa for the threaded implant

(Fig 11). For the model with a cortical bone graft block, maximal von Mises stresses were registered mesial to the second premolar; these were 28.7 MPa for the cylindrical implant and, mesial to the first molar, 25.5 MPa for the threaded implant (Table 3).

With regard to the x-load simulation (laterotrusion), similar stress behaviors were observed within the complex and simplified implant models. A significant difference was registered for the distribution of stresses with and without a bone graft block (Fig 12). In the model without a cortical bone graft block, maximal stress values in the surrounding alveolar bone in the buccal first molar were 10.69 MPa for the cylindrical implant and 10.41 MPa for the threaded dental implant. In the model with a cortical bone graft block, the maximal von Mises stress values in the palatal second premolar area were 10.31 MPa for the cylindrical implant, while those in the buccal first molar area were 9.71 MPa for the threaded implant (Table 3).

Distribution of von Mises Stresses

The four models featured different geometries in the interior sinus. Therefore, the meshes and numbers of elements differed. To render the models comparable, a statistical approach was used for evaluation. Von Mises stresses of each bony component were retrieved separately, evaluated with respect to maximum values, and transformed into histograms as well as cumulative plots to illustrate the differences between models.

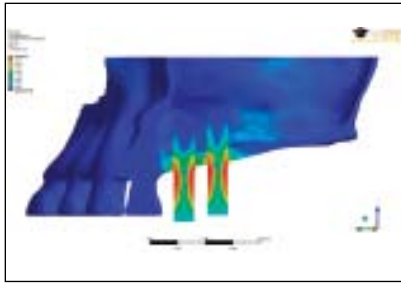


Fig 10 Distribution of von Mises stresses from protrusion (y-load) within cylindrical implants, without bone graft block. The maximal von Mises stress is 78.8 MPa.

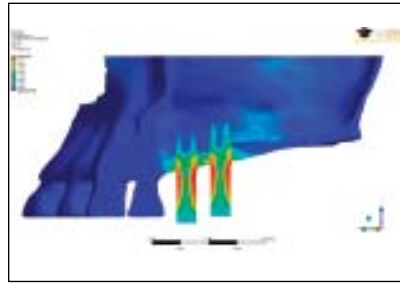


Fig 11 Distribution of von Mises stresses from protrusion (y-load) within threaded implants without a cortical bone graft block. The maximal von Mises stress is 83.1 MPa.

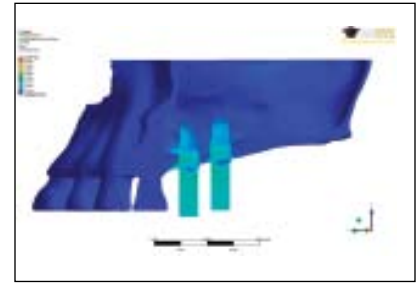


Fig 12 Distribution of von Mises stresses from laterotrusion (x-load) without a cortical bone graft block in the threaded implant model.

Table 3 Maximal Values for von Mises Stresses (MPa) in Alveolar Bone

Model	Masticatory strength (z)	Protrusion (y)	Laterotrusion (x)
Without cortical bone graft block + cylindrical implant	17.55	31.55	10.69
Without cortical bone graft block + threaded implant	20.2	38.17	10.41
With cortical bone graft block + cylindrical implant	11.78	28.7	10.31
With cortical bone graft block + threaded implant	8.3	25.5	9.71

The stress distributions in the alveolar bone of the maxilla are shown on the basis of classical histograms in Fig 13. The lines in the graphics indicate mean stress values. Without a bone graft block, the stress distributions and mean values shifted to the right, indicating the presence of greater stresses for all loads.

The same distribution behavior is shown in cumulative distribution diagrams in Figs 14 to 16. The shift of distribution is shown in greater detail in the maxillary alveolar bone in Fig 14, and the stress distribution in the augmented bone region only is shown in Fig 15. In all cases, the models with a cortical bone graft block featured more stress values in the lower MPa range and fewer high stress values. The opposite was the case when no cortical bone graft block was used: fewer low-stress values were seen, and more stress values in the upper MPa range were observed. These results confirm that the inserted bone graft block absorbs stresses. Comparison of the dental implant and the cylindrical implant showed an exact overlay of the two curves (Fig 16).

DISCUSSION

The sinus elevation technique has significantly extended the indications for implant placement in the maxilla in the presence of an alveolar crest that is 5 mm or thinner. With an alveolar crest thickness of less than 3 mm, primary stability of implants is frequently not achieved.

A modified method of sinus elevation employs a cortical bone graft block for additional implant stabilization.^{10–13} The present authors performed an FE analysis to evaluate and compare the standard sinus bone graft method with the modified approach. A patient-specific 3D model based on CT data for the left half of the maxilla with augmentation and the cortical bone graft block was generated and used in settings of different complexity.

Many FE studies of the posterior maxilla with sinus augmentation are based on block-shaped anatomical models that show principal stress concentrations.^{14,15,17–19} The current 3D models simulate the entire complex anatomy of the left maxilla, facial skeleton, and augmented sinus. The 3D FE model was segmented and designed using the CT data of a patient who had received this modified sinus bone graft and was provided with virtually inserted dental implants. With regard to basic conditions, as a limitation of this FE study, it was assumed that complete osseointegration of the implants had been achieved. In practice, the complex mechanical behavior of natural and augmented craniofacial structures may be affected differently.

Natural conditions as well as occlusal forces must be considered when seeking optimal biomechanical conditions for simulation of implants.^{18,20–23} In addition to the magnitude of the chewing forces, the direction from which they act on the implant and the surrounding bone is also important. During simulation in the

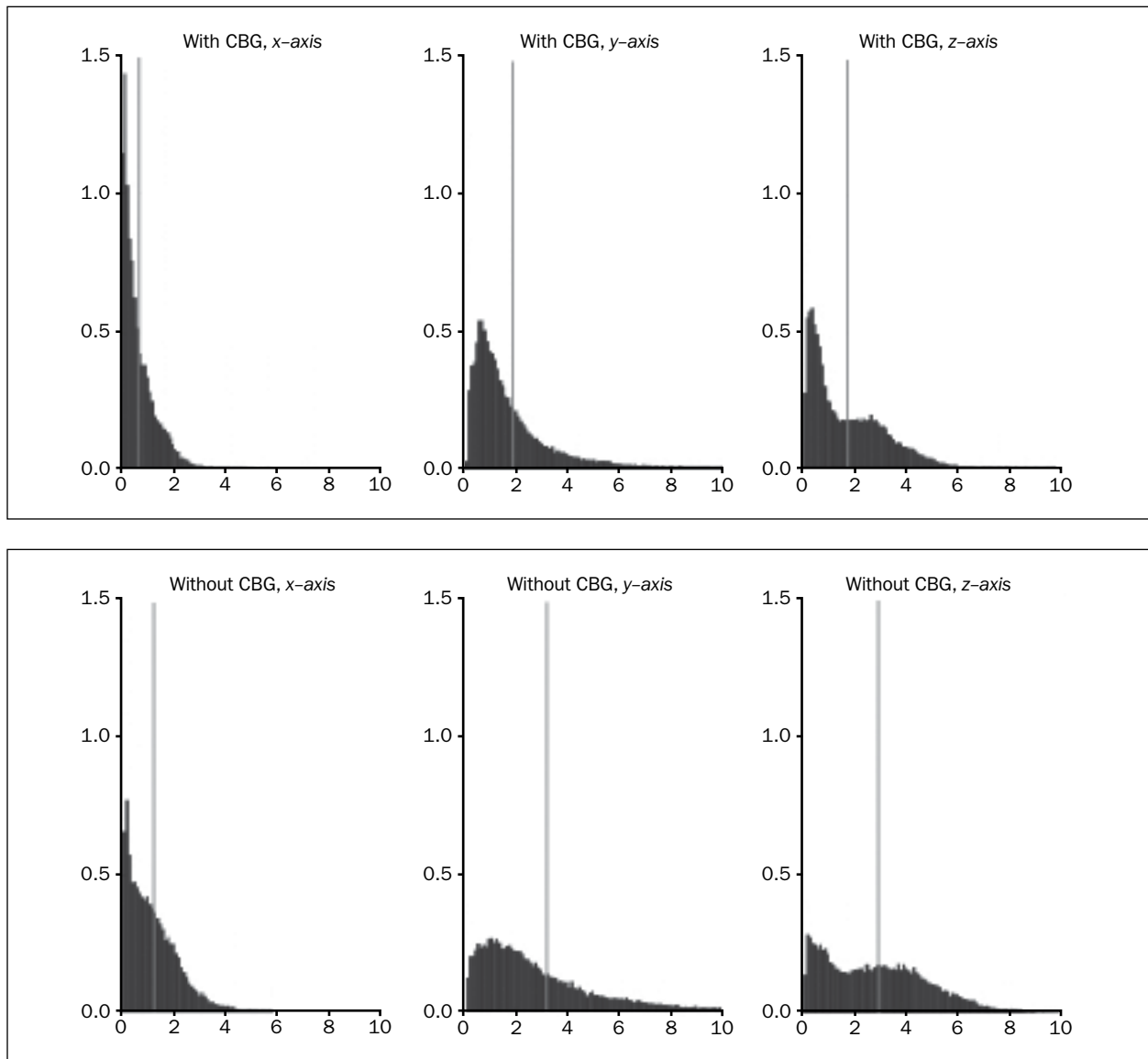


Fig 13 Von Mises stress distribution histograms resulting from x-, y- and z-loads in the maxilla bone implants with threads and with and without cortical bone graft block (CBG). The lines in the histograms indicate mean values; x = laterotrusion; y = protrusion; z = masticatory strength.

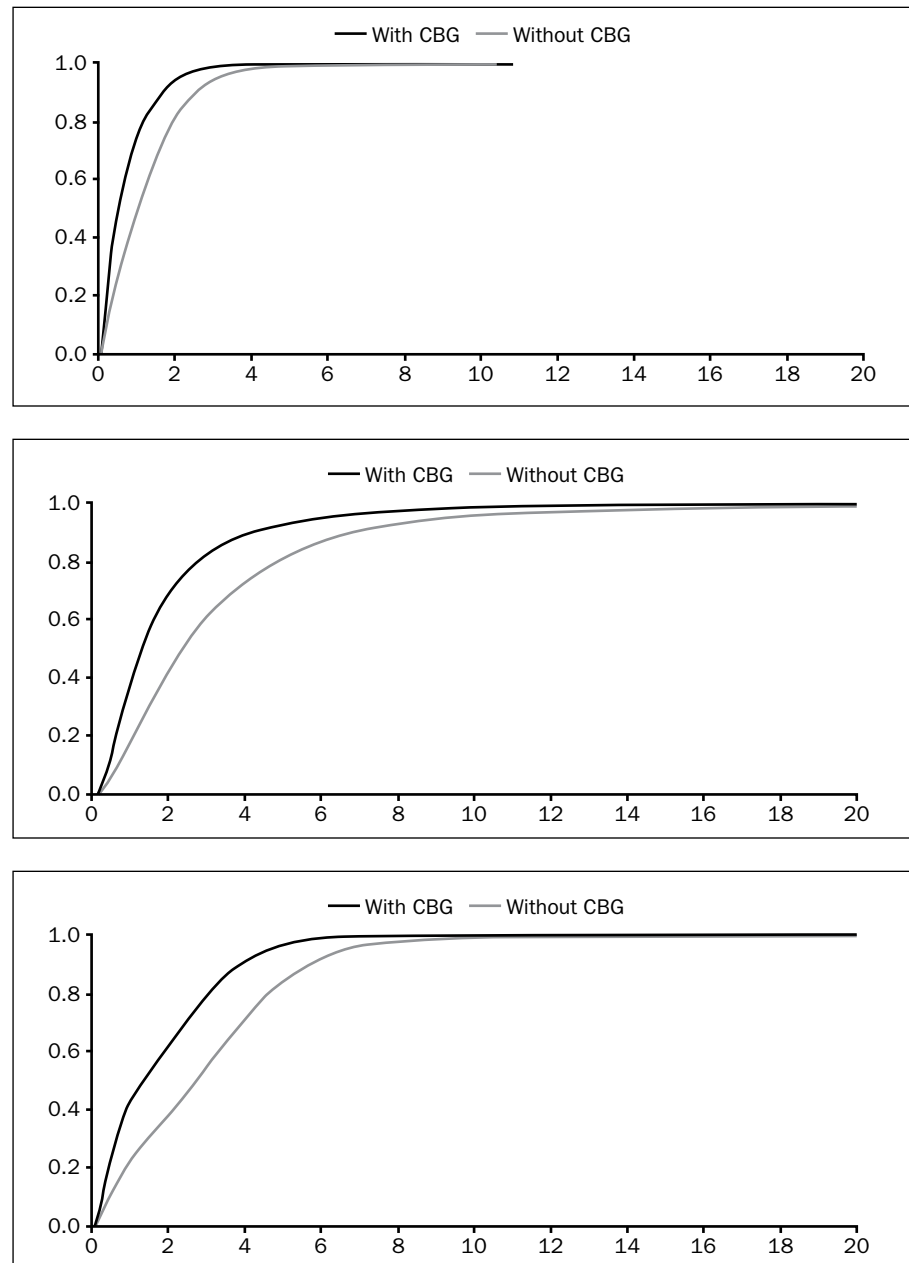
z-axis (masticatory strength), the maximal von Mises stress in the alveolar bone surrounding the implant neck was about 20 MPa in the model without a cortical bone graft block and about 12 MPa in the model with a cortical bone graft block. When loads were exerted in alignment with the axis, the forces on the cortical bone of the maxilla were absorbed and transferred. Force transmission within the augmented area was minimal. During laterotrusion (x-axis), the tension reached about 10 MPa. Maximum stress values of approximately 38 MPa were achieved during protrusion (y-axis) without a cortical bone graft block. These loads triggered a lever effect, which exerted stress on the augmented region. The modified method produced

lower stresses. This is similar to bicortical anchorage, such as that typically achieved in the anterior region of the mandible, and enhances stability.

The maximum von Mises stress seen in the implant was about 80 MPa. Titanium tolerates stresses ranging up to 900 MPa without irreversible deformation. The force of 80 MPa is within the range of tolerance and thus should not contribute to mechanical implant failure.

According to Frost's law,²⁴⁻²⁶ a stress of 1 to 2 MPa induces remodeling, 3 to 20 MPa induces modeling, and 20 MPa is the threshold for microscopic damage. The stress of masticatory strength and laterotrusion—8 to 17 MPa—is within the range of bone modeling. However, in the model without a cortical bone graft block,

Fig 14 Cumulative distribution of von Mises stresses in the maxilla bone resulting from (top to bottom) x-, y-, and z-loading of threaded implants with and without CBG.



the observed maximal stress value of approximately 38 MPa in protrusion was within the range of bone microdamage. The stress value for the model with a cortical bone graft block was significantly lower (25 MPa). Generally, the highest stresses are concentrated on the interface between the implant neck and the surrounding cortical bone. In long-term radiographic and FE studies, bone loss around the implant neck has been reported for loaded implants.^{17,27-32} This is in agreement with the present results. It also indicates that bone resorption would be lower in this area if a cortical block were used.

At stresses above 20 MPa, microdamage to bone is known to stimulate repair by bone remodeling (re-

ferred to as A-R-F, for the three cellular stages of bone remodeling: Activation of osseous precursor cells, Resorption, and Formation).³³ This is achieved by positive feedback mechanisms involving remodeling that is stimulated to repair damage.³⁴ Bone is probably equipped with a control system to maintain mechanical homeostasis. This leads to resorption of alveolar bone at the implant neck, which is the region of highest stress, and also contributes to the stability of resorption and bone remodeling. One of the important conclusions drawn from this study is that the cortical bone graft block absorbs and reduces stress significantly in the cortical bone, particularly at the implant neck (Table 3).

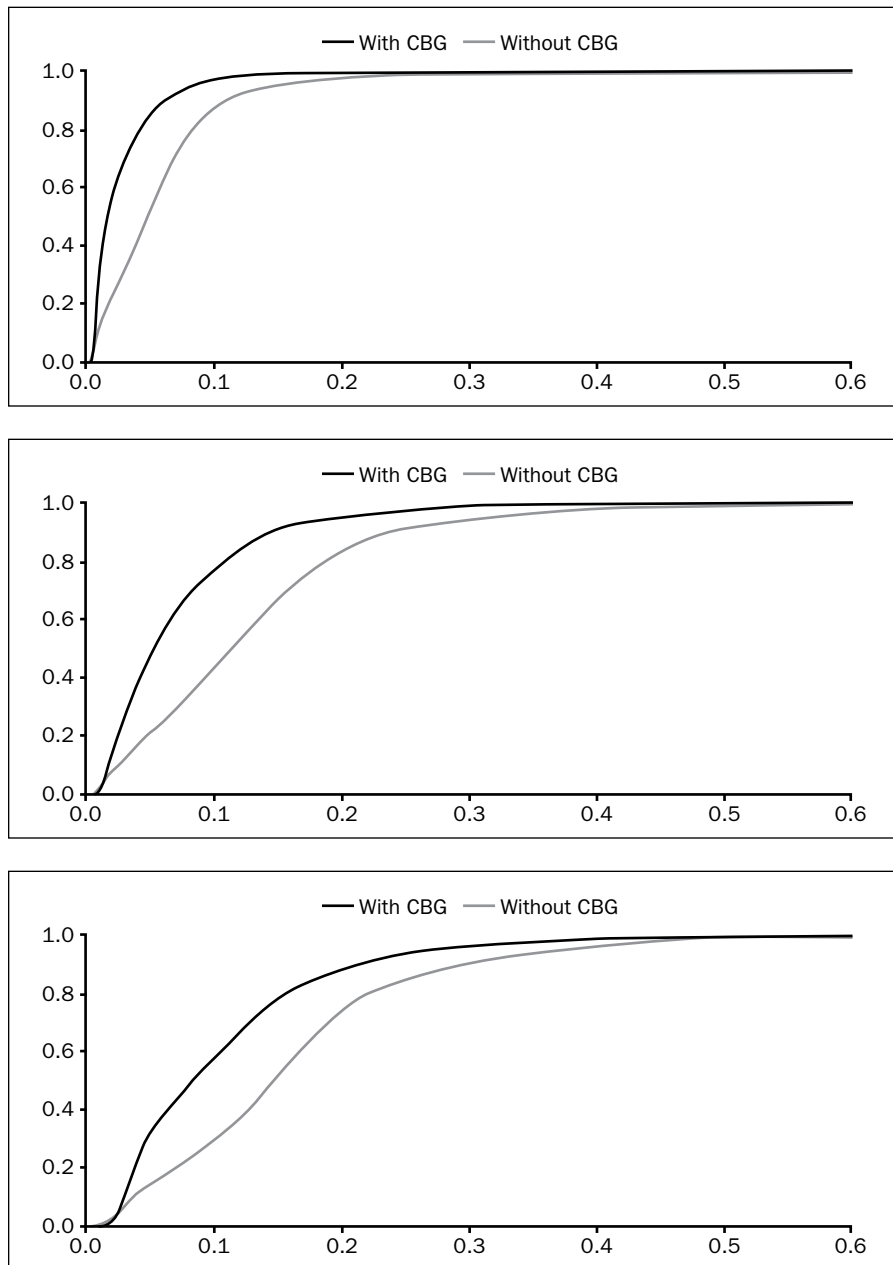


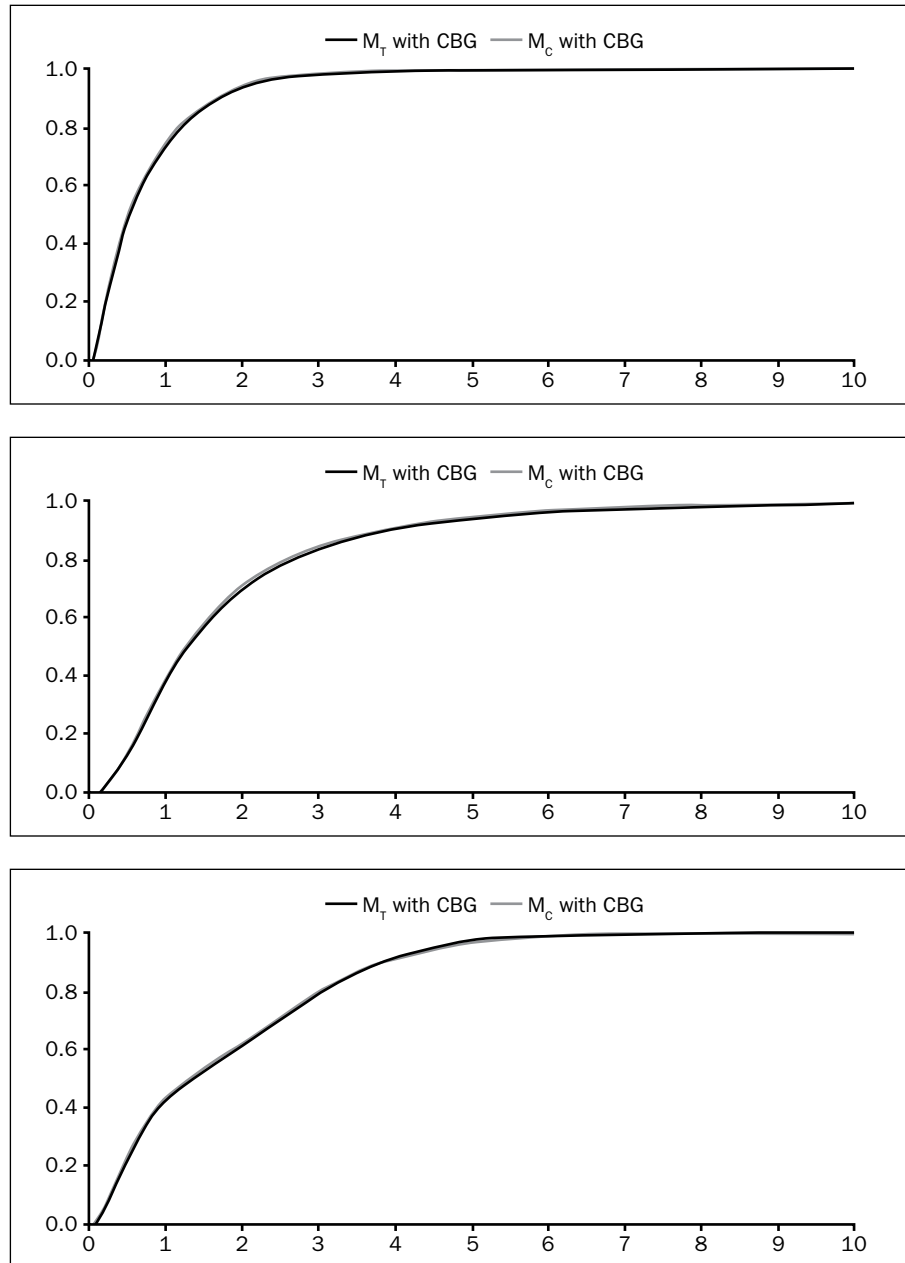
Fig 15 Cumulative distribution of von Mises stresses in the augmented bone resulting from (top to bottom) x-, y-, and z-loading with and without CBG for threaded implants.

Complex models with threaded implants showed some singularities. Numeric singularities and instabilities are well known issues of FE simulations with complex geometries.³⁵ These may occur at areas of transition from one material to another, especially from a material with a high Young's modulus to that with a significantly lower one. This is true for the transition zone from titanium to cortical bone as well as titanium to cancellous bone and leads to von Mises stress peaks in titanium, whereas cortical and cancellous bone plasticize according to their natural characteristics. To deal with this problem, only the von Mises stresses of cortical and cancellous bone were measured, as the stress

within the titanium implant was not the focus of the present study. Furthermore, the models with cylindrical implant approximations were free of singularities and showed the same stress behavior as the complicated models. Hence, there is no need to generate models encompassing the complexity of real dental implants to achieve realistic simulations of stress distributions in cortical and cancellous bone.

The magnitude of maximal von Mises stress obviously differs from those registered in simulations with cylindrical implants, especially for z-loads (masticatory strength). The Young's modulus of cortical bone appears to possess high stiffness, while cancellous bone

Fig 16 Cumulative distribution of von Mises stresses resulting from (top to bottom) x-, y-, and z-loading of the maxilla with threaded (M_T) and unthreaded-cylindrical (M_C) implants with CBG.



is marked by low stiffness. Embedment of a cancellous bone graft block in cancellous augmentation material reduces the difference in the Young's modulus and stabilizes the augmented area. Therefore, the quality of the graft is of great concern when the quantity of existing cancellous maxillary bone is limited.¹⁵

The absorption of stress secondary to the cortical bone graft block was reflected in significant shifts of stress distribution (Figs 13 to 15). The equivalent behavior of the simulations was demonstrated with a complex 3D model using a threaded implant model and a simplified model based on a cylindrical approximation (Fig 16).

ACKNOWLEDGMENTS

The project was supported by the Austrian Science Fund FWF L526-B05. The authors thank Schoellerbank Austria and the Salzburg branch office of the Austrian Society of Dentistry, Oral and Maxillofacial Diseases (Österreichischen Gesellschaft für Zahn-, Mund-, und Kieferheilkunde). The study was approved by the Ethics Committee of Salzburg (Ethikkommission für das Bundesland Salzburg, no. 415-E803/3-2007).

REFERENCES

- Cawood JI, Howell RA. A classification of the edentulous jaws. *Int J Oral Maxillofac Surg* 1988;17:232–236.
- Boyne PJ, James RA. Grafting of the maxillary sinus floor with autogenous marrow and bone. *J Oral Surg* 1980;38:613–616.
- Blomqvist JE, Albers P, Isaksson S. Two-stage maxillary sinus reconstruction with onosseous implants: A prospective study. *Int J Oral Maxillofac Implants* 1998;13:758–766.
- Fugazzotto PA, Vlassis J. Long-term success of sinus augmentation using various surgical approaches and grafting materials. *Int J Oral Maxillofac Implants* 1998;13:52–58.
- Jensen OT, Shulman LB, Block MS, Iacono VJ. Report of the sinus consensus conference of 1996. *Int J Oral Maxillofac Implants* 1998;13(suppl):11–45.
- Schaaf H, Streckbein P, Lendeckel S, et al. Sinus lift augmentation using autogenous bone grafts and platelet-rich plasma: Radiographic results. *Oral Surg Oral Med Oral Pathol Oral Radiol Endod* 2008;106:673–678.
- Watzek G, Weber R, Bernhart T, Ulm C, Haas R. Treatment of patients with extreme maxillary atrophy using sinus floor augmentation and implants: Preliminary results. *Int J Oral Maxillofac Surg* 1998;27:428–434.
- Wheeler SL, Holmes RE, Calhoun CJ. Six-year clinical and histologic study of sinus-lift grafts. *Int J Oral Maxillofac Implants* 1996;11:26–34.
- Valentini P, Abensur D. Maxillary sinus floor elevation for implant placement with demineralized freeze-dried bone and bovine bone (Bio-Oss): A clinical study of 20 patients. *Int J Periodontics Restorative Dent* 1997;17:232–241.
- Chaushu G, Mardinger O, Calderon S, Nissan J. The use of cancellous allograft for sinus floor augmentation with simultaneous implant placement in the posterior atrophic maxilla. *J Periodontol* 2009;80:422–428.
- Krekmanov L, Heimdahl A. Bone grafting to the maxillary sinus from the lateral side of the mandible. *Br J Oral Maxillofac Surg* 2000;38:617–619.
- Khoury F. Augmentation of the sinus floor with mandibular bone block and simultaneous implantation: A 6-year clinical investigation. *Int J Oral Maxillofac Implants* 1999;14:557–564.
- Jensen J, Sindet-Pedersen S. Autogenous mandibular bone grafts and osseointegrated implants for reconstruction of the severely atrophic maxilla: A preliminary report. *J Oral Maxillofac Surg* 1991;49:1277–1287.
- Lin CL, Chang SH, Chang WJ, Kuo YC. Factorial analysis of variables influencing mechanical characteristics of a single tooth implant placed in the maxilla using finite element analysis and the statistics-based Taguchi method. *Eur J Oral Sci* 2007;115:408–416.
- Fanuscu MI, Vu HV, Poncelet B. Implant biomechanics in grafted sinus: A finite element analysis. *J Oral Implantol* 2004;30:59–68.
- Himmlova L, Dostalova T, Kacovsky A, Konvickova S. Influence of implant length and diameter on stress distribution: A finite element analysis. *J Prosthet Dent* 2004;91:20–25.
- Koca OL, Eskitascioglu G, Usumez A. Three-dimensional finite-element analysis of functional stresses in different bone locations produced by implants placed in the maxillary posterior region of the sinus floor. *J Prosthet Dent* 2005;93:38–44.
- Tepper G, Haas R, Zechner W, Krach W, Watzek G. Three-dimensional finite element analysis of implant stability in the atrophic posterior maxilla: A mathematical study of the sinus floor augmentation. *Clin Oral Implants Res* 2002;13:657–665.
- Chang CL, Chen CS, Hsu ML. Biomechanical effect of platform switching in implant dentistry: A three-dimensional finite element analysis. *Int J Oral Maxillofac Implants* 2010;25:295–304.
- Mericske-Stern R, Venetz E, Fahrlander F, Burgin W. In vivo force measurements on maxillary implants supporting a fixed prosthesis or an overdenture: A pilot study. *J Prosthet Dent* 2000;84:535–547.
- Borcic J, Anic I, Smojver I, Catic A, Miletic I, Ribaric SP. 3D finite element model and cervical lesion formation in normal occlusion and in malocclusion. *J Oral Rehabil* 2005;32:504–510.
- Morneburg TR, Proschel PA. In vivo forces on implants influenced by occlusal scheme and food consistency. *Int J Prosthodont* 2003;16:481–486.
- Proeschel PA, Morneburg T. Task-dependence of activity/bite-force relations and its impact on estimation of chewing force from EMG. *J Dent Res* 2002;81:464–468.
- Frost MH. Wolff's Law and bone's structural adaptations to mechanical usage: An overview for clinicians. *Angle Orthod* 1994;64:175–188.
- Frost MH. Bone's mechanostat: A 2003 update. *Anat Rec* 2003;275A:1081–1101.
- Frost MH. Update of bone physiology and Wolff's law for clinicians. *Angle Orthod* 2004;74:3–15.
- Adell R, Lekholm U, Rockler B, Brånemark PI. A 15-year study of osseointegrated implants in the treatment of the edentulous jaw. *Int J Oral Surg* 1981;10:387–416.
- Henry P, Bower RC, Woolridge JA. Radiographic evaluation of marginal bone height around titanium implants [abstract]. *J Dent Res* 1988;67:629.
- Pikner SS, Grondahl K, Jemt T, Friberg B. Marginal bone loss at implants: A retrospective, long-term follow-up of turned Brånemark system implants. *Clin Implant Dent Relat Res* 2009;11:11–23.
- Jemt T, Johansson J. Implant treatment in the edentulous maxillae: A 15-year follow-up study on 76 consecutive patients provided with fixed prostheses. *Clin Implant Dent Relat Res* 2006;8:61–69.
- Snauwaert K, Duyck J, van Steenberghe D, Quirynen M, Naert I. Time dependent failure rate and marginal bone loss of implant supported prostheses: A 15-year follow-up study. *Clin Oral Investig* 2000;4:13–20.
- Wiltfang J, Schultze-Mosgau S, Nkenke E, Thorwarth M, Neukam FW, Schlegel KA. Onlay augmentation versus sinus lift procedure in the treatment of the severely resorbed maxilla: A 5-year comparative longitudinal study. *Int J Oral Maxillofac Surg* 2005;34:885–889.
- Roberts WE, Turley PK, Breznjak N, Fiedler PJ. Implants: Bone physiology and metabolism. *CDA J* 1987;15:54–61.
- Brunski JB. In vivo bone response to biomechanical loading at the bone/dental-implant interface. *Adv Dent Res* 1999;13:99–119.
- Terrier A, Buchler P, Farron A. Bone-cement interface of the glenoid component: Stress analysis for varying cement thickness. *Clin Biomech (Bristol, Avon)* 2005;20:710–717.